Effect of Etching Time on Sensing Behavior of Porous Silicon Prepared by Electrochemical Method

Abbas A. Abbas [1]
Saba J. Hasan [1]
Inaam M. Abdulmajeed [2]
Salah Q. Hazaa [3]

[1] *Department of Physics, College of Education, Mustansiriyah University, Baghdad, IRAQ*
[2] *Department of Physics, College of Science, University of Baghdad, Baghdad, IRAQ*
[3] *Department of Medical Physics, College of Science, Al-Karkh University for Sciences, Baghdad, IRAQ*

In the current work, porous silicon (PS) was prepared using an electrochemical etching process in a solution of hydrofluoric acid (HF) and ethanol (C_2H_5OH) at constant current density and various etching times using p-type silicon with a (100) orientation and resistivity of 8 Ω.cm. The structural and topographical characteristics of the prepared samples were introduced by the x-ray diffraction patterns and atomic force microscopy. Also, the sensing characteristics of the prepared samples to ammonia gas vapor was introduced. Cubic structure was confirmed in all porous samples. The PS layer on the silicon wafer was growing and the grain size within this layer was increasing with etching time. Average roughness, root-mean-square roughness, photoluminescence peak intensity, and a minor shift to higher frequency (blue shift) were increased with decreasing average grain size.

Keywords: Porous silicon; Photoluminescence; Gas sensors; Electrochemical method
Received: 18 September 2023; **Revised:** 08 November; **Accepted:** 15 November 2023

1. Introduction

The topic of porous silicon (PS) and its structures is becoming more popular in science and technology due to their large surface-to-volume ratio, ease of formation by various etching processes on various crystalline silicon substrates, and control of the surface morphology [1]. It is largely utilized in photovoltaic, biomedical, and sensing applications because it can provide a range of etching conditions by adjusting a number of variables such as current density, etching time, HF acid concentration, and illumination conditions [1,2][1-4]. Porous silicon can be produced by several methods depending on the desired structures and properties [5]. Porous silicon is often prepared using one of two techniques: chemical etching in HF solution or electrochemical etching. The distinction between the two methods is that external bias is used during electrochemical etching [3][6,7]. Porous silicon has been used as gas sensors for nitrogen dioxide (NO_2) [4-6], carbon monoxide (CO) [7], hydrogen [8-10], ethanol and heptane vapors [10,11], carbon dioxide (CO_2) [11] and others.

The main purpose of this work is to investigate the sensing performance of porous silicon as a cost-effective, simple and high sensitivity gas sensor for ammonia (NH_3) gas vapor.

2. Experimental Part

The electrochemical etching was performed on a (100)-oriented p-type silicon wafer, with electrical resistivity of 8 Ω.cm at constant current density of 10 mA/cm^2, and various etching times (5, 10, 15 and 20 min) to produce porous silicon layers. The electrolyte solution used for this process is a 1:2 mixture of ethanol (C_2H_5OH) and hydrofluoric acid (HF). According to the gravimetric data of the prepared samples, the porosity of the PS was calculated.

The x-ray diffraction patterns were recorded using a SHIMADZU 6000 X-Ray Diffractometer to introduce the crystalline structures of the prepared porous silicon samples. A LiCuix 3205N system was used to record the photoluminescence (PL) spectra. The surface topography of the prepared samples was examined using a CSPM AA3000 atomic force microscope (AFM). In order to examine the sensing properties of the prepared PS samples, they were placed inside a testing system, which consists of a chamber, control heater, vacuum system (a rotary pump) to a work at rough vacuum of 50 mbar, ohmmeter to measure the resistance of the samples and thermocouple to read sample temperature. The sensing test was performed on the PS samples using the measurement of the resistance of PS in air (R_a) and in presence of ammonia gas (R_g), and the results were recorded for different operating temperatures (30-400°C) using a constant concentration of ammonia gas (20 ppm).

 © ALL RIGHTS RESERVED

3. Results and Discussion

The XRD patterns were recorded in the range of 2θ between 25° and 35°. The XRD patterns of crystalline silicon (c-Si) and porous silicon (PS) prepared at various etching durations and constant current densities are shown in Fig. (1). According to ICDD N 1997 and 2011 JCPDS data, this figure shows that the c-Si has a strong and narrow peak at 2θ=28.43° corresponding to the (111) plane direction of Si of cubic structure. Large particle size and good crystallinity are indicated by the narrow peak. The peak along (111) slightly shifts to a lower angle than the bulk Si peak, as shown in table (1), indicating that the cubic silicon surface has formed pores. The creation of a porous structure on the crystalline silicon surface is shown by the widening of this peak when the etching time is increased [12].

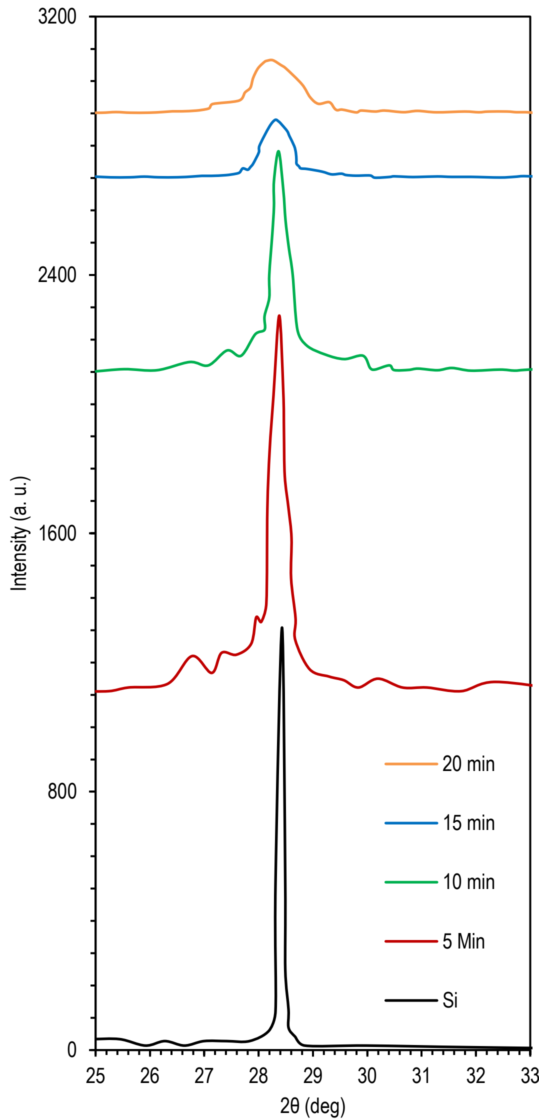

Fig. (1) XRD patterns of PS and c-Si prepared after different etching times

Crystallite size (D) was calculated using the Scherrer's formula (Eq. 1) [13] and summarized in table (1)

$$D = \frac{0.9\,\lambda}{\beta\cos\theta} \quad (1)$$

where λ is the wavelength of x-ray (in nm), β is the FWHM (in radians) and θ is the diffraction angle.

As shown from table (1), the values of crystallite size decreases as etching time is increased and nanoscale dimensions were achieved for all etching times. These results are in agreement with previously published works [14,15].

In Fig. (2), the topography of PS samples prepared after different etching times is depicted by the AFM images. It shows how the PS is constructed similarly to a sponge. The average grain size, average roughness, and root-mean-square roughness of these samples are shown in table (2). The results show that the average grain size decreases as etching time is increased, while the average roughness and root-mean-square (r.m.s.) roughness are increased. This variation might be caused by the decrease in the quantity of holes on the silicon surface. This behaviour complies perfectly with [16,17].

Table (1) Structural parameters for c-Si and PS prepared after different etching times

Etching time (min)	2θ Exp. deg	$d_{(111)}$ Std. Å	$d_{(111)}$ Exp. (Å)	D (nm)
Before etching	28.43	3.135	3.1369	82.2
5	28.38		3.1423	74.4
10	28.36		3.1435	59.5
15	28.30		3.1510	45.6
20	28.26		3.1554	35.7

The percentage content of voids in the PS layer is referred to as silicon's "P" porosity and is computed gravitationally using Eq. (2) [18,19] as well as stated in table (2)

$$P = \frac{m_1 - m_2}{m_1 - m_3}\,100\% \quad (2)$$

where m_1, m_2, and m_3 are, respectively, the masses of the c-Si, PS, and PS following the removal of the PS layer (which is accomplished by dipping it for a few minutes in an aqueous solution of KOH). The outcome demonstrated that the porosity increases as etching time is increased. This outcome is explained by an increase in the width and quantity of pores.

Table (2) AFM parameters and porosity of PS samples prepared after different etching times

Etching Time (min)	Average Grain Size (nm)	Average Roughness (nm)	RMS (nm)	P (%)
5	82	0.461	0.498	28.9
10	75	1.105	1.340	45.6
15	56	10.28	12.50	55.7
20	43	11.90	14.80	65.4

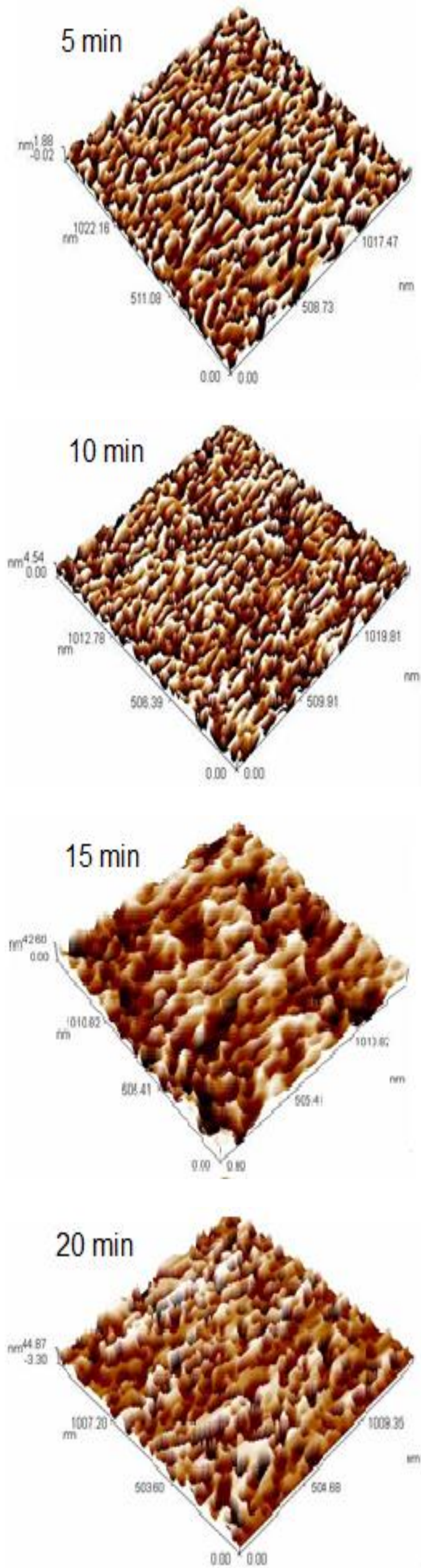

Fig. (2) AFM images of PS samples prepared after different etching times

Shorter wavelengths have high energy to induce the photoluminescence (PL) in the prepared samples. Therefore, the PL spectra were recorded as the prepared samples were excited with radiation source whose wavelength is shorter than the emission wavelength. Figure (3) displays these PL spectra for PS sample prepared after different etching times and a constant current density of 10 mA/cm^2. These spectra clearly show that the PL intensity increases as the etching time is increased and a small blue shift is observed. This effect might be attributed to the decrease in crystallite size and increase in porosity [3,20].

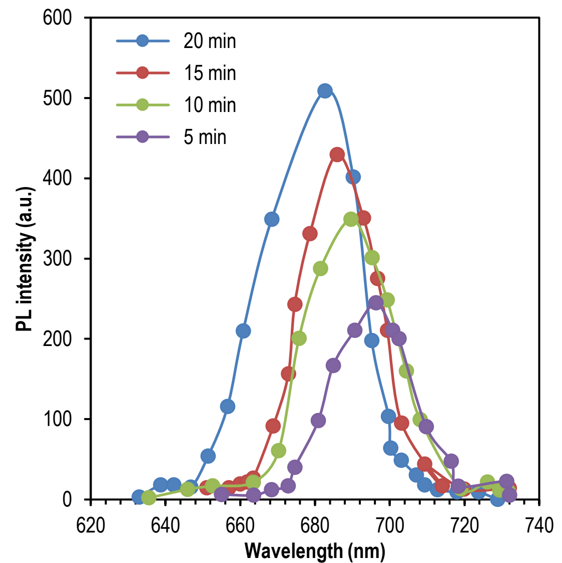

Fig. (3) PL spectra of the PS samples prepared after different etching times

Using Eq. (3), the energy gap (E_g) of the preared PS samples was determined and shown in table (3). It should be observed that these values are greater than the energy gap of p-type Si (1.11eV), and they also increase from 1.775 to 1.814 eV as the etching time is increased. These values are within the range 1.5-2.5 eV achieved by previously published works [21-24].

$$E_g = \frac{hc}{\lambda_{max}} \quad (3)$$

where λ_{max} is the wavelength at maximum intensity of the PL spectrum, and h is Planck's constant

Table (3) Values of energy gap and PL emission wavelength for PS samples prepared after different etching times

Etching time (min)	λ (nm)	E_g (eV)
5	696	1.78
10	690	1.79
15	686	1.81
20	683	1.82

The sensing behavior of PS samples was investigated as a function of the operation temperature. The gas sensing property of the PS samples were tested using ammonia gas at a concentration of 20 ppm. Humans can tolerate

 © ALL RIGHTS RESERVED

ammonia gas at a concentration of about 25 ppm [25], hence it is crucial that the sensor respond to concentrations below this limit [26]. Sensitivity (S) is the ratio of the change in sensor resistance upon exposure to NH_3 gas (R_g) to that sensor's resistance in air (R_a). It was calculated using the following relation as [27-29]

$$S = \left[\frac{R_g - R_a}{R_a}\right] \times 100\% \qquad (4)$$

In reference [4], the sensitivity of PS samples as a function of operating temperature (30-400°C) was depicted. The study revealed that the sensitivity of all samples has increased as operating temperature is increased up to 200°C before decreasing as operating temperature went higher. The gas sensitivity decreases with increasing temperature because beyond 200°C, the surface would be unable to oxidize the gas and the NH_3 may burn before reaching the surface of the pores. The results also indicate that the sensitivity is higher for the PS samples prepared after longer etching times. This is due to their huge surface area, higher NH_3 gas oxidation rate, higher surface roughness, and larger grain size [30].

In order to develop sensors for the necessary applications, response and recovery times are crucial factors. The sensitivity must be high and the response and recovery times must be short for a gas sensor to be effective. The response and recovery times of a PS sample exposed to 20 min etching and 10 mA/cm^2 current density at different operating temperatures and 20 ppm NH_3 are shown in Fig. (5). The operating temperature was seen to have an effect on both times. At higher operating temperatures, the response and recovery times are shortened. This might be attributed to the increase in the surface reaction rate at higher temperatures because of sufficient thermal energy of the sensor material. Nevertheless, it was discovered that at all operating temperatures, response time was faster than recovery time. A faster rate of gas oxidation may have caused the faster response.

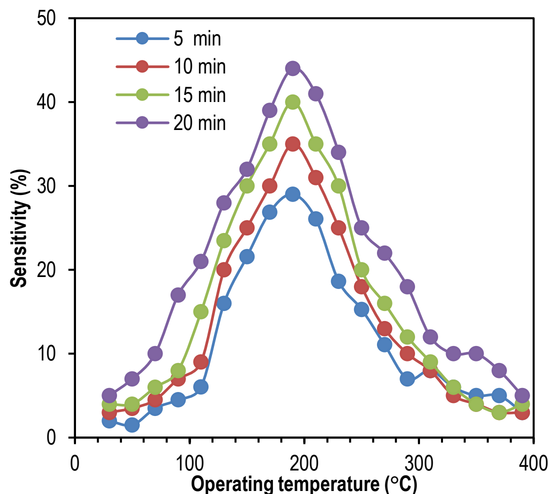

Fig. (4) Variations of gas sensitivity of PS samples with operating temperature

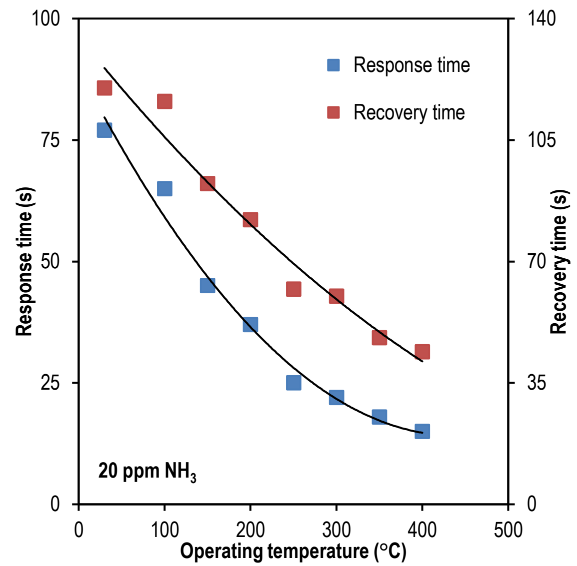

Fig. (5) Variations of response and recovery times of PS sample prepared after 20min etching time with operating temperature

4. Conclusions

Chemical etching was effectively employed to prepare porous silicon samples and the etching time had a significant effect on the structure and topography of these samples. As etching time was increased, porosity, energy gap, and crystallite size have increased. The sample prepared after 20min etching time showed the highest sensitivity at 200°C operating temperature with response/recovery times 37s/82s when exposed to ammonia gas at a concentration of 20 ppm, rather than any longer etching time that necessitated additional research.

References

[1] [1] K.A. Salman, K. Omar and Z. Hassan, “The effect of etching time of porous silicon on solar cell performance”, *Superlatt. Microstruct.*, 50(6) (2011) 647-658.

[2] M.H. Kareem, M. Adi and H.T. Hussein, “The effect of current density on the properties of porous silicon gas sensor for ethanol and methanol vapour detection”, *J. Appl. Sci. Nanotech.*, 1(4) (2021) 52-60.

[3] O.A. Hammadi, “Magnetically-supported electrically-induced formation of silicon carbide nanostructures on silicon substrate for optoelectronics applications”, *Opt. Quantum. Electron.*, 54(7) (2022) 427.

[4] F.J. Kadhim, O.A. Hammadi and A.A. Anber, “Spectroscopic study of chromium-doped silicon nitride nanostructures prepared by DC reactive magnetron sputtering”, *Iraqi J. Appl. Phys.*, 17(2) (2021) 11-14.

[5] O.A. Hammadi “Conjunctional Freezing-Assisted Ultrasonic Extraction of Silicon Dioxide Nanopowders from Thin Films Prepared by Physical Vapor Deposition Technique”, *Iraqi J. Appl. Phys.*, 15(4) (2019) 23-28.

 © ALL RIGHTS RESERVED

[6] D.T.J. Ee, C.K. Sheng and M.I.N. Isa, "Photoluminescence of porous silicon prepared by chemical etching method", *Malaysian J. Anal. Sci.*, 15(2) (2011) 227-231.
[7] O.A. Hammadi, M.K. Khalaf and F.J. Kadhim, "Farbication of UV photodetector from nickel oxide nanoparticles deposited on silicon substrate by closed-field unbalanced dual magnetron sputtering techniques", *Opt. Quantum Electron.*, 47(12) (2015) 3805-3813.
[8] C.H. Qing et al., "The light-enhanced NO_2 sensing properties of porous silicon gas sensors at room temperature", *Chin. Phys. B*, 21(5) (2012) 58201-58205.
[9] C. Baratto et al., "A novel porous silicon sensor for detection of sub-ppm NO_2 concentrations", *Sens. Actuat. B,* 77 (2001) 62-66.
[10] S. Chakane, A. Gokarna and S.V. Bhoraskar, "Metallophthalocyanine coated porous silicon gas sensor selective to NO_2", *Sens. Actuat. B*, 91 (2003) 1-5.
[11] C. Baratto et al., "Gas Detection with a porous silicon based sensors", *Sens. Actuat. B*, 65 (2000) 257-259.
[12] K. Luong, A. Sine and S. Bhansali, "Devlopment of a highly sensitive porous Si-based hydrogen sensor using Pd nanostructures", *Sens. Actuat. B*, 111-112 (2005) 125-129.
[13] R. Angelucci et al., "Permieated porous silicon for hydrocarbon sensor fabrication", *Sens. Actuat. A*, 74 (1999) 95-99.
[14] R. Liu et al., "Novel porous silicon vapor sensor based on polarization interferometry", *Sens. Actuat. B*, 87 (2002) 58-62.
[15] M. Rocchi et al., "Sensing CO_2 in a chemically modified porous silicon film", *phys. stat. sol.*, 197(2) (2003) 365-369.
[16] V.S. Vidhya et al., "Development of porous silicon matrix and characteristics of porous silicon/tin oxide structures", *J. Non-Cryst. Sol.*, 357 (2011) 1522-1526.
[17] S.Q. Haza'a and H.R. Shaker, "Effect of thickness on structural, optical and sensing properties of SnS thin films prepared by ultrasonic nebulizer method", *J. Multidiscip. Eng. Sci. Technol.*, 4(9) (2017) 8241-8249.
[18] C.A.C. Abdullah et al., "Structural and optical properties of N-type and P-type porous silicon produced at different etching time", *Int. J. Electroactive Mater.,* 7 (2019) 28-37.
[19] R. Ramadan and R.J. Martín-Palma, "The infiltration of silver nanoparticles into porous silicon for Improving the performance of photonic devices", *Nanomaterials*, 12 (2022) 271- 284.
[20] H.H. Hussein, "Study of the characteristics of porous silicon by electrochemical etching", *Eng. Technol. J.*, 31(1) (2013) 34-38.
[21] R.G. Kadhim, R.A. Ismail and W.M. Abdulridha, "Structural, morphological, chemical and optical properties of porous silicon prepared by electrochemical etching", *Int. J. Thin Films Sci. Technol.*, 4(3) (2015) 199-203.
[22] F. Alfeel et al., "Using AFM to determine the porosity in porous silicon", *J. Mater. Sci. Eng. A*, 2(9) (2012) 579-583.
[23] L.A. Aslanov et al., "Nanosilicon stabilized with ligands: Effect of high-energy electron beam on luminescent properties", *Surf. Interface Anal.*, 52(12) (2020) 957-961.
[24] C.K. Sheng and D.T.J. Ee, "Photoluminescence, morphological and electrical properties of porous silicon formulated with different HNO_3 concentrations", *Resul. In Phys.*, 10 (2018) 5-9.
[25] M. Rajabim and R.S. Dariani, "Current improvement of porous silicon photovoltaic devices by using double layer porous silicon structure: applicable in porous silicon solar cells", *J. Porous Mater.*, 16 (2009) 513-519.
[26] M. Bahar, H. Eskandari and N. Shaban, "Electrical properties of porous silicon for n2 gas sensor", *J. Theor. Comput. Sci.*, 4(1) (2017) 1-6.
[27] A. Mortezaali, S.R. Sani and F.J. Jooni, "Correlation between porosity of porous silicon and optoelectronic properties", *J. Non-Oxide Glasses*, 1(3) (2009) 293-299.
[28] Ş. Doğan et al., "Porous silicon: volume-specific surface area determination from AFM measurement data", *J. Mater. Sci. Eng. B*, 3(8) (2013) 518-523.
[29] H. Nanto, T. Minami and S. Takata, "Zinc-oxide thin-film ammonia gas sensors with high sensitivity and excellent selectivity", *J. Appl. Phys.*, 60(2) (1986) 482-484.
[30] A.J. Rodrgíuez et al., "A Fiber Optic Ammonia Sensor Using a Universal pH Indicator", *Sensors*, 14 (2014) 4060-4073.
[31] S.Q. Haza'a, H.R. Shaker and N.A. Al-Hamadan, "Effect of Thickness on Structural, Electrical and Gas Sensing Properties of CdS Thin Films Prepared by Ultrasonic Nebulizer Method", *J. Iraqi Al-Khwarizmi Soc. (JIKhS)*, 2(2) (2018) 1-14.
[32] I.A. Abbas, S.Q. Hazaa and S.H. Salman, "Employment of Titanium dioxide thin film on NO_2 gas sensing", *J. Phys.: Conf. Ser.*, 3 (2021) 1-7.
[33] L.V. Duy et al., "Room Temperature Ammonia Gas Sensor Based on p-Type-like V_2O_5 Nanosheets towards Food Spoilage Monitoring", *Nanomaterials*, 13 (2023) 146-164.
[34] M.H. Kareem, A.M. Abdul Hussein and H.T. Hussein, "Effect of current density on the porous silicon preparation as gas sensors" *J. Mech. Behav. Mater.*, 10 (2021) 2021-2027.

 © ALL RIGHTS RESERVED